Volume 13
Number 12
28 March 2022
Pages 3303–3612

# Chemical Science

rsc.li/chemical-science

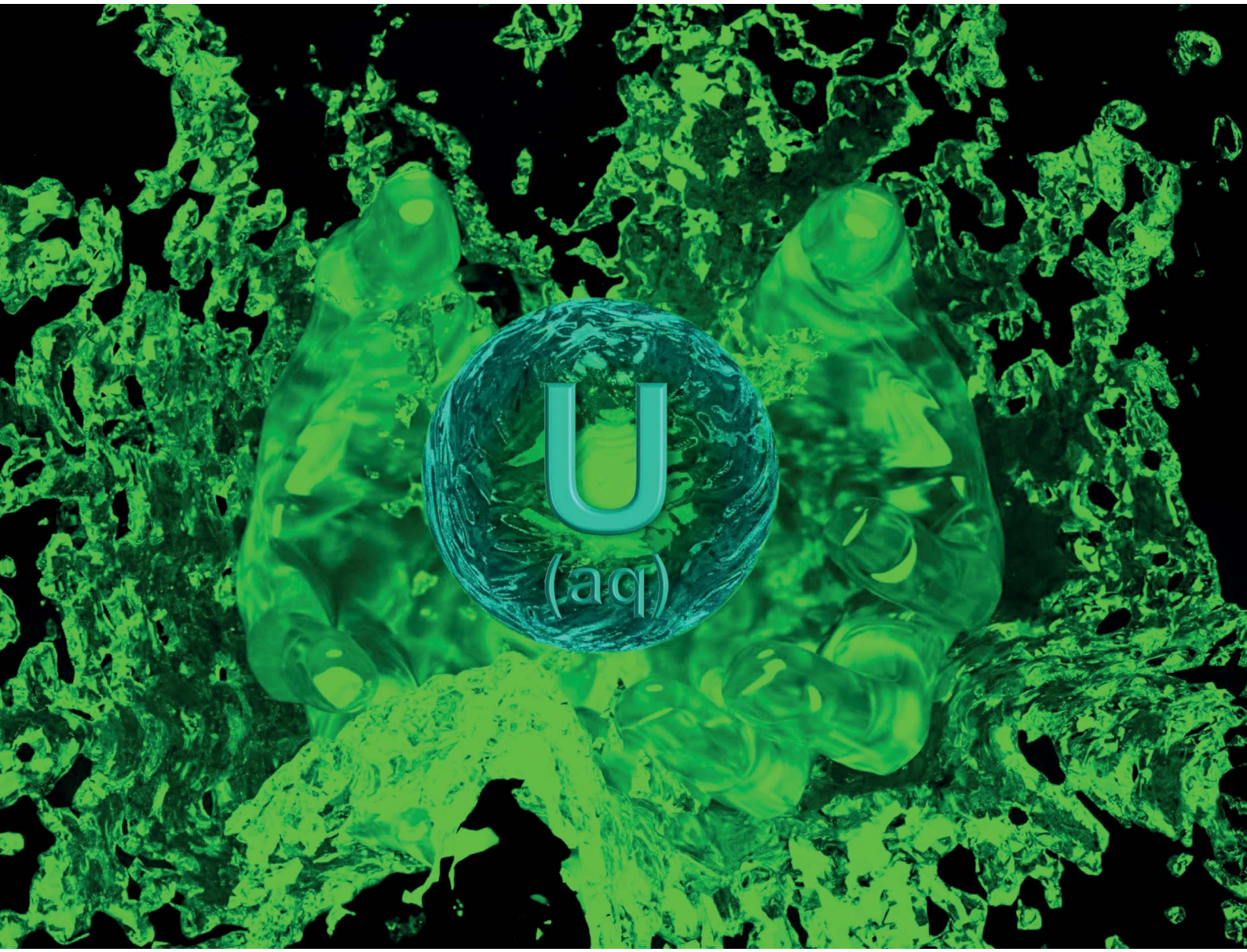


ISSN 2041-6539

ROYAL SOCIETY OF CHEMISTRY

**EDGE ARTICLE**

Gabriel Ménard *et al.*

Selective electrochemical capture and release of uranyl from aqueous alkali, lanthanide, and actinide mixtures using redox-switchable carboranes

Chemical Science

ROYAL SOCIETY OF CHEMISTRY

EDGE ARTICLE

View Article Online
View Journal | View Issue





Cite this: *Chem. Sci.*, 2022, **13**, 3369

All publication charges for this article have been paid for by the Royal Society of Chemistry

Received 19th December 2021
Accepted 20th February 2022

DOI: 10.1039/d1sc07070c

rsc.li/chemical-science

# Selective electrochemical capture and release of uranyl from aqueous alkali, lanthanide, and actinide mixtures using redox-switchable carboranes†

Megan Keener, ‡[a] Maxwell Mattejat,‡[a] Shao-Liang Zheng,[b] Guang Wu,[a] Trevor W. Hayton[a] and Gabriel Ménard *[a]

We report the selective electrochemical biphasic capture of the uranyl cation ($UO_2^{2+}$) from mixed-metal alkali ($Cs^+$), lanthanide ($Nd^{3+}$, $Sm^{3+}$), and actinide ($Th^{4+}$, $UO_2^{2+}$) aqueous solutions to an organic, 1,2-dichloroethane (DCE), phase using the *ortho*-substituted *nido*-carborane anion, $[1,2\text{-}(Ph_2PO)_2\text{-}1,2\text{-}C_2B_{10}H_{10}]^{2-}$ ($^{PO}Cb^{2-}$). The reduced $^{PO}Cb^{2-}$ is generated by electrochemical reduction of the *closo*-carborane, $^{PO}Cb$, prior to mixing with the aqueous mixed-metal solution. Subsequent $UO_2^{2+}$ release from the captured product, $[UO_2(^{PO}Cb)_2]^{2-}$, was performed by galvanostatic bulk electrolysis of the DCE phase and back-extraction of $UO_2^{2+}$ to a fresh aqueous phase. The selective capture and release of $UO_2^{2+}$ was confirmed by combined ICP-OES and NMR spectral analyses of the aqueous and organic phases, respectively, against the newly synthesized *nido*-carborane complexes, $[[CoCp^*_2][Cs(^{PO}Cb)]]_2$, $[CoCp^*_2]_3[Nd(^{PO}Cb)_3]$, $[CoCp^*_2]_3[Sm(^{PO}Cb)_3]$, and $[CoCp^*_2]_2[Th(^{PO}Cb)_3]$.

## Introduction

With over 440 operational reactors worldwide, nuclear energy currently provides 11% of all electricity. Several countries have proposed to increase nuclear energy production to meet their Paris Agreement targets for decarbonizing their economies, with the most ambitious being India and China that propose eight- and five-fold increases in domestic nuclear capacity, respectively.[1] While nuclear energy is often considered a low-carbon energy alternative to fossil fuels,[2,3] the disposal of spent nuclear fuel (SNF), as well as the inadvertent release of radioactive material to the environment (*e.g.*, release of $^{137}Cs$ at Chernobyl and Fukushima), make this technology imperfect.

Uranium, in its dioxide form ($UO_2$), is both the main component in nuclear fuel, as well as SNF, where the concentration drops to approximately 95%. New fission products generated include: Pu (0.9%); the minor actinides (0.1% (Np, Am, Cm)); lanthanides, Tc, Mo, I, Cs and others (together *ca.* 4%).[4] As of 2020, approximately 450 000 tons of SNF have been cumulatively generated worldwide, of which only ~25% have been reprocessed using the decades-old Plutonium Uranium Redox EXtraction (PUREX) process.[5] While this commercial, liquid–liquid process is extremely efficient at extracting and recycling $UO_2^{2+}$ using stoichiometric extractants, in turn reducing SNF loads, PUREX involves the selective extraction of a pure Pu stream which raises significant proliferation concerns from major stakeholders, such as the U.S.[6] While other reprocessing schemes addressing these concerns have been developed (*e.g.*, UREX), none are commercial. To this day, proliferation concerns have superseded reprocessing efforts in places like the U.S., forcing countries to instead increase their SNF storage capacity, thus deferring action on the nuclear waste issue.[4,6,7] New strategies for the selective separation and recovery of $UO_2^{2+}$ from SNF, without the parallel extraction of a Pu stream, could therefore significantly aid in reducing net SNF generated from reactors, minimizing demands on long-term geological repositories, and in turn closing the fuel cycle.

We recently reported a new, biphasic, electro/chemical method for capturing $UO_2^{2+}$ using the *ortho*-substituted *nido*-carborane anion, $[1,2\text{-}(Ph_2PO)_2\text{-}1,2\text{-}C_2B_{10}H_{10}]^{2-}$ ($^{PO}Cb^{2-}$) generating the captured species, $[UO_2X_n(^{PO}Cb)_{(2-n/2)}]^{2-}$ ($n = 0$, 2; X = Cl, OAc; Fig. 1a). Electrochemical oxidation of this species was initiated to generate the oxidized *closo*-carborane ($^{PO}Cb$), initiating the release of $UO_2^{2+}$ to the aqueous layer. Repeated capture and release of $UO_2^{2+}$ in monophasic organic solution further demonstrated the potential applicability and recyclability of this extractant.[8] In this study, we wanted to explore the *selective* biphasic capture and release of $UO_2^{2+}$ using the $^{PO}Cb^{2-}/^{PO}Cb$ system from aqueous solutions of alkali, lanthanide, and actinide metals more closely mimicking SNF streams. The choice of metals, and the reasons for using each, are as follows: (1) natural abundance $^{133}Cs^+$ (100%) was used to mimic the highly

[a]*Department of Chemistry and Biochemistry, University of California, Santa Barbara, California 93106, USA. E-mail: menard@chem.ucsb.edu*

[b]*Department of Chemistry and Chemical Biology, Harvard University, Cambridge, Massachusetts 02138, USA*

† Electronic supplementary information (ESI) available: Synthesis, electrochemical details, NMR, UV-vis, XRD data. CCDC 2071514–2071518. For ESI and crystallographic data in CIF or other electronic format see DOI: 10.1039/d1sc07070c

‡ These authors contributed equally to this work.

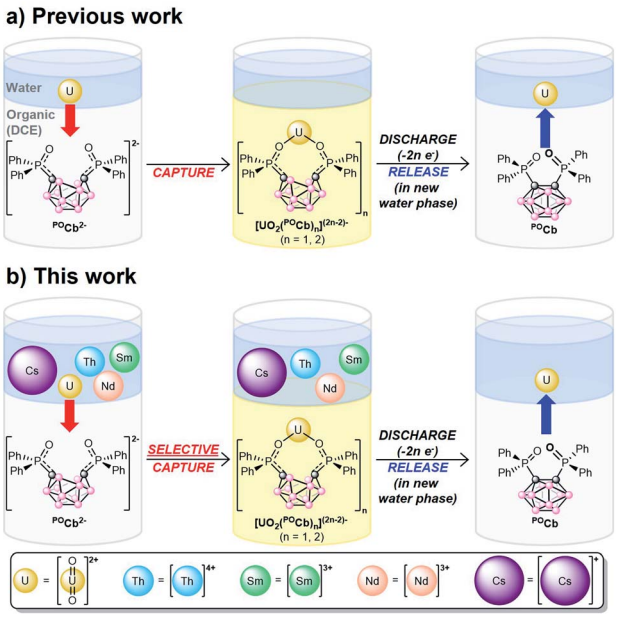


Fig. 1 (a) Our previous work demonstrating the biphasic, electrochemical capture and release of $UO_2^{2+}$ using the $^{PO}Cb^{2-}/^{PO}Cb$ system. (b) This work highlighting the *selective* capture and release of $UO_2^{2+}$ from aqueous solutions containing alkali, lanthanide, and actinide metals.

radiotoxic $^{137}Cs$ isotope which is responsible for much of the human health, environmental, and hot SNF disposal issues;[7,9,10] (2) $Nd^{3+}$ and $Sm^{3+}$ were chosen due to their abundance in SNF;[7] (3) $Th^{4+}$ was used due to its abundance in SNF,[7] and also because it functions as a $Pu^{4+}$ surrogate in light of our inability to handle this highly controlled element in house.[11–13] Herein, we describe both the coordination chemistry of $^{PO}Cb^{2-}$ to these individual metals, as well as the *highly selective* electrochemical capture of $UO_2^{2+}$ with $^{PO}Cb^{2-}$ from the mixed-metal aqueous solution to an organic phase. The electrochemical release of $UO_2^{2+}$ to a fresh aqueous phase is also described (Fig. 1b).

## Results and discussion

The coordination chemistry of the $^{PO}Cb^{2-}$ ligand was investigated using the previously reported $[CoCp^*_2]^+$ salt, $[CoCp^*_2]_2[^{PO}Cb]$ ($Cp^* = \eta^5\text{-}C_5Me_5$),[8] in tandem with the nitrate salts of $Cs^+$, $Nd^{3+}$, $Sm^{3+}$, and $Th^{4+}$. All complexes were synthesized following an analogous synthetic procedure in MeCN. The Cs complex was generated by addition of an equimolar solution of $[CoCp^*_2]_2[^{PO}Cb]$ to a solution of $CsNO_3$ in MeCN at r.t. Following the selective recrystallization and separation of the $[CoCp^*_2][NO_3]$ byproduct, the desired product was isolated and unambiguously identified by single crystal X-ray diffraction (XRD) studies as the dimeric salt, $[[CoCp^*_2][Cs(^{PO}Cb)]]_2$ (Fig. 2a). The symmetric dimer features a central diamond-shaped core structure with two Cs atoms at the apical positions held in place by oxide donors from each ligand (Cs1–O(1, 1′) = 2.9893(18), 3.0844(19) Å), as well as Cs–H–B bonds[14,15] (Cs1–B(3, 3′) = 3.681(3), 3.631(3) Å; Cs1–H(3, 3′) = 2.924, 3.08(3) Å). Other interactions outside the diamond core are provided by the additional oxide donor (Cs1–O2 = 2.9356(18) Å), as well as an additional B contact (Cs1–B4′ = 3.726(3) Å). We note that a Cs–H (3.199 Å) contact arising from a phenyl *meta*-C–H bond of an adjacent dimer is also observed, generating a polymeric structure (see Fig. S7† (not shown in Fig. 2a)). The *nido* $^{PO}Cb^{2-}$ ligand charged state is maintained as indicated by the long C1–C2 distance (2.862 Å),[8] which is well outside the range of a C–C bond. Together, we tentatively assign a coordination number (CN) of 9 to the large Cs cation. Due to the imposed crystal symmetry, identical bond metrics are found for Cs1′. The bonding types and lengths, the polymeric structure, and the assigned CN are similar to previously reported data for Cs.[14–17] Lastly, while the solid-state structure displays inequivalent P=O donor groups in the $^{PO}Cb^{2-}$ ligands, we note that the diamagnetic complex displays a single resonance in the $^{31}P$ NMR spectrum at 31.7 ppm in MeCN-$d_3$ indicating higher symmetry in solution, perhaps due to the breakup of the polymeric structure initiated by the coordinating solvent (Fig. S10†).

The lanthanide ($Nd^{3+}$, $Sm^{3+}$) and actinide ($Th^{4+}$) complexes were next synthesized using an identical procedure. Three equivalents of $[CoCp^*_2]_2[^{PO}Cb]$ were added to one equivalent of $M(NO_3)_n$ (M = Nd, Sm ($n$ = 3); Th ($n$ = 4)) in MeCN at r.t. The $[CoCp^*_2][NO_3]$ byproduct was again selectively crystallized and separated prior to isolation of the final products, which were all unambiguously identified by single crystal XRD studies as: $[CoCp^*_2]_3[Nd(^{PO}Cb)_3]$ (Fig. S8†); $[CoCp^*_2]_3[Sm(^{PO}Cb)_3]$

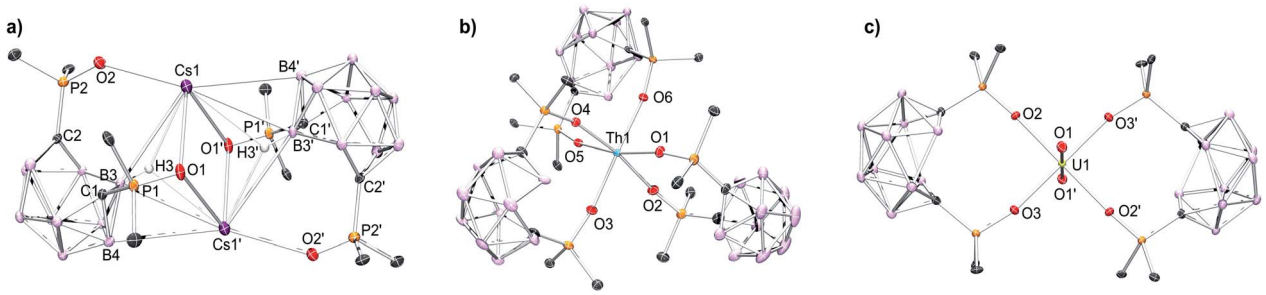


Fig. 2 Solid-state molecular structures obtained by XRD studies of: (a) $[[CoCp^*_2][Cs(^{PO}Cb)]]_2$; (b) $[CoCp^*_2]_2[Th(^{PO}Cb)_3]$, and; (c) $[CoCp^*_2]_2[UO_2(^{PO}Cb)_2]$.[8] $[CoCp^*_2]^+$ counter cations, phenyl C–H linkages, co-crystallized solvent molecules, and all H atoms, except those shown in (a), are omitted for clarity. Pertinent bond lengths and angles are discussed in the manuscript. The polymeric structure of $[[CoCp^*_2][Cs(^{PO}Cb)]]_2$ (a), filling an additional coordination site at Cs, is shown in Fig. S7.†

(Fig. S9†), and; $[CoCp^*_2]_2[Th(^{PO}Cb)_3]$ (Fig. 2b). All complexes have a central 6-coordinate metal center in pseudo-octahedral geometries. Average M–O bond distances of 2.327 Å (Nd), 2.315 Å (Sm), and 2.297 Å (Th) are similar to reported values[18–24] and follow an expected periodic trend based on decreasing ionic radii and increasing ionic charge (for Th). Long carborane C–C distances (average 2.86 Å) in each case are again indicative of a *nido* $^{PO}Cb^{2-}$ configuration.[8] The solid-state structure of the previously reported uranyl complex, $[CoCp^*_2]_2[UO_2(^{PO}Cb)_2]$, is also shown in Fig. 2c as a comparison to the new complexes reported here.[8] Spectroscopically, $[CoCp^*_2]_3[Nd(^{PO}Cb)_3]$ and $[CoCp^*_2]_3[Sm(^{PO}Cb)_3]$ display $^{31}$P NMR resonances at 140.6 and 27.9 ppm, respectively. These values are notably different from each other, likely due to their varying paramagnetism. These values are also much different from the diamagnetic $[CoCp^*_2]_2[Th(^{PO}Cb)_3]$ (51.3 ppm) and $[CoCp^*_2]_2[UO_2(^{PO}Cb)_2]$ (52.0 ppm) complexes.[8]

Building on our previous work (Fig. 1a),[8] we investigated the selective electrochemical capture of $UO_2^{2+}$ from mixed aqueous alkali ($Cs^+$), lanthanide ($Nd^{3+}$, $Sm^{3+}$), and actinide ($Th^{4+}$, $UO_2^{2+}$) solutions mimicking in part SNF. Mixed-metal aqueous stock solutions were first prepared by dissolving equimolar quantities of the common starting materials, $CsNO_3$, $Nd(NO_3)_3(THF)_3$, $Sm(NO_3)_3(THF)_3$, $Th(NO_3)_4(H_2O)_x$, and $UO_2(NO_3)_2(THF)_2$ in Milli-Q deionized water, either with a NaOAc buffer (0.5 M, pH = 5.2) or without (pH = 2.6). The buffer in the former was used for two reasons: (1) to mimic our previous results which required the use of a buffer to control for the pH-dependent extinction coefficient ($\varepsilon$) of $UO_2^{2+}$ which was monitored by UV-vis spectroscopy,[8,25,26] and; (2) to compare the extraction efficacy of our system at varying pH values. In contrast to our previous work, we used inductively-coupled plasma optical emission spectrometry (ICP-OES) to directly, and more accurately, measure trace metal concentrations in the aqueous phases pre-extraction (pre-X), post-extraction (post-X), and following back-extraction (back-X, *vide infra*).

Three separate 1,2-dichloroethane (DCE) solutions were next loaded with $^{PO}Cb$ (1 equiv.), [PPN][$PF_6$] (0.5 equiv. $[PPN]^+ = [Ph_3P{=}N{=}PPh_3]^+$) as internal standard for NMR spectroscopy (*vide infra*), and [$Bu_4N$][$PF_6$] (0.1 M) as supporting electrolyte, and were loaded into one of two compartments of divided H-cells. Each counter compartment was loaded with a heterogeneous carbon additive (Ketjenblack) which served as a capacitive buffer[8,27] and which was mixed in DCE with 0.1 M [$Bu_4N$][$PF_6$]. All H-cells were configured with physical glass-frit separators and contained reticulated vitreous carbon electrodes on each side (see ESI† for full experimental detail and H-cell setup). We note that each of these experiments were run in triplicate. The $^{PO}Cb$ solutions were electrochemically reduced by galvanostatic bulk electrolysis (GBE) to a theoretical state-of-charge (SOC) of *ca.* 77% assuming a 100% coulombic efficiency (Fig. S5†). Subsequent analyses of the carborane solutions by unlocked $^{31}P\{^1H\}$ NMR spectroscopy revealed the clean conversion of $^{PO}Cb$ to the reduced *nido*-carborane, $^{PO}Cb^{2-}$, each in approximate 76% yield and in line with the SOC. We note a loss of *ca.* 10% of combined carborane resonances ($^{PO}Cb$ and $^{PO}Cb^{2-}$) following charging and relative to the starting solutions and internal standard, perhaps due to ill-defined electrochemical side reactions. Each charged solution was then removed from its respective H-cell and mixed with either: (1) a non-buffered (pH = 2.6) aqueous mixed-metal solution with *ca.* 1.25 equiv. of each metal relative to $^{PO}Cb^{2-}$ (Fig. 3a); (2) a NaOAc-buffered (pH = 5.2) aqueous mixed-metal solution with *ca.* 1.25 equiv. of each metal relative to $^{PO}Cb^{2-}$ (Fig. 3b), or; (3) a NaOAc-buffered (pH = 5.2) aqueous mixed-metal solution with *ca.* 0.60 equiv. of each metal relative to $^{PO}Cb^{2-}$ (Fig. 3c). Significant yellowing of the organic phases was observed after 1.5 h of rapid biphasic mixing (Fig. 1b).

The aqueous mixed-metal phases were analyzed by ICP-OES prior to mixing with the organic phases (pre-X), following biphasic mixing (post-X), as well as following back-X (*vide infra*). Analysis of the non-buffered solution (Fig. 3a) post-X revealed an average decrease in $UO_2^{2+}$ concentration of 20.7%, with minimal observed changes to the concentrations of $Th^{4+}$, $Nd^{3+}$, $Sm^{3+}$, and $Cs^+$ relative to pre-X. The minor decreases in the concentrations of these latter metals were within error to the observed changes in the controls, which were performed in parallel using identical aqueous and organic solutions (but without added $^{PO}Cb$ or $^{PO}Cb^{2-}$), as observed by the hashed bars in Fig. 3a–c. In contrast to this non-buffered solution, analysis of the buffered solution containing *ca.* 1.25 equiv. of each metal (Fig. 3b) post-X revealed an improved extraction of $UO_2^{2+}$ with an average decrease in concentration of 59.7% relative to pre-X (note that the pre-X [$UO_2^{2+}$] reached saturation here at a slightly lower concentration than the other metals). While extraction of $Th^{4+}$, $Nd^{3+}$, $Sm^{3+}$, and $Cs^+$ also increased here relative to the non-buffered solution, the observed changes were again within error and consistent with the control experiments, thus suggesting that the observed extraction of these ions was not driven by coordination to $^{PO}Cb^{2-}$. We next probed the effect of modifying the $^{PO}Cb^{2-}$ : metal ratios. We note that the observed ratios of $^{PO}Cb^{2-}$ : $UO_2^{2+}$ are either 1 : 1 (ref. 8) ($Cs^+$ also, Fig. 2a) or 2 : 1 (Fig. 2c), whereas all other complexes reported here ($Th^{4+}$, $Sm^{3+}$, $Nd^{3+}$) are 3 : 1. Reducing the mixed-metal aqueous buffered solution concentration to *ca.* 0.6 equiv. of each metal to $^{PO}Cb^{2-}$ revealed an increased post-X extraction of $UO_2^{2+}$ – 71.6% relative to pre-X (Fig. 3c) – compared to the 1.25 equiv. extraction (Fig. 3b). While no significant changes in $Nd^{3+}$, $Sm^{3+}$, and $Cs^+$ concentrations were observed here relative to the controls, we did observe a slight decrease in $Th^{4+}$ concentration (9.2% *vs.* pre-X) which was greater than the control (1.6%) and beyond the detection error limit. While these data suggest that $^{PO}Cb^{2-}$ may drive the extraction of some $Th^{4+}$ under these higher ratios, the selectivity for $UO_2^{2+}$ under these conditions still dominates, as evidenced by the calculated separation factor (*SF*), derived from the distribution ratios of metals: $SF_{U/Th} = 25$.[28]

In each experiment, the organic phases were analyzed by $^{31}P\{^1H\}$ NMR spectroscopy prior to GBE, following GBE, following extraction (post-X stage), following GBE discharge (*vide infra*), and following back-X (see Fig. S2–S4† for representative spectra). A representative post-X spectrum is shown in Fig. 3d and revealed the formation of (integrated ratios relative to initially formed $^{PO}Cb^{2-}$ are in parentheses): a main product at 52.0 ppm (54%), residual $^{PO}Cb$ (18%), and minor new byproduct

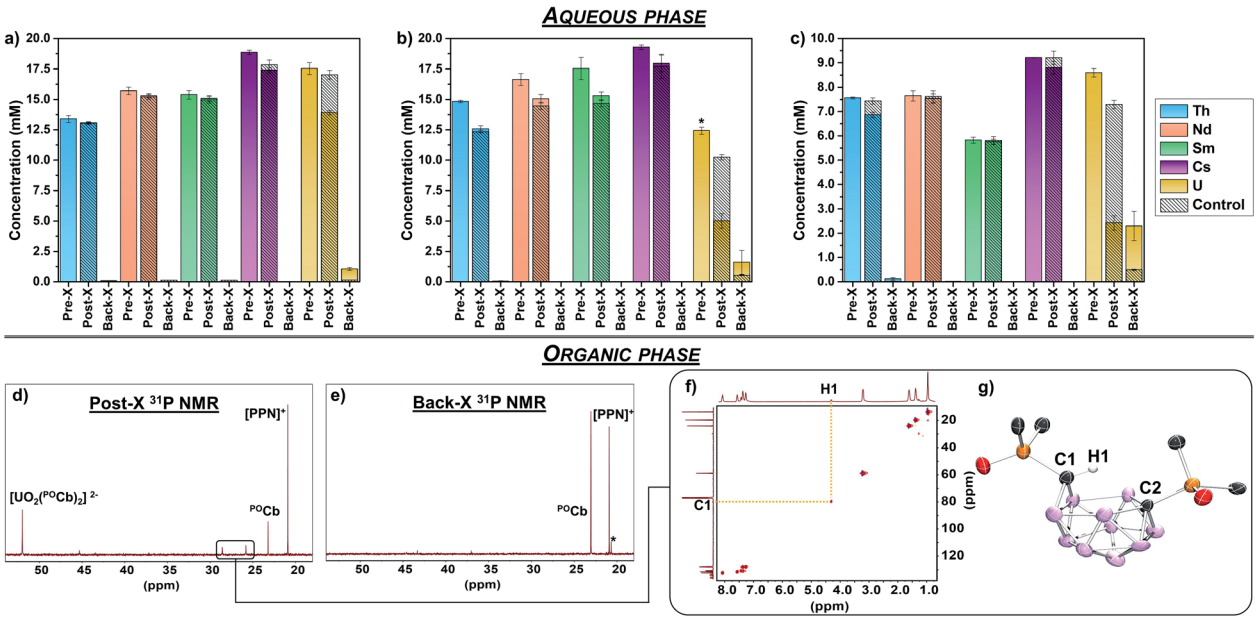


Fig. 3 ICP-OES, spectroscopic, and crystallographic data for the selective electrochemical capture and release of $UO_2^{2+}$ from mixed-metal ($Cs^+$, $Nd^{3+}$, $Sm^{3+}$, $Th^{4+}$, $UO_2^{2+}$) aqueous solutions using the $^{PO}$**Cb**/$^{PO}$**Cb**$^{2-}$ system in DCE. (a–c) Average concentrations (from triplicate runs) of each metal species initially (pre-X) and following post-X and back-X using the following conditions and assuming 1.0 equiv. of $^{PO}$**Cb**$^{2-}$: (a) a non-buffered (pH = 2.6) aqueous mixed-metal solution with *ca.* 1.25 equiv. of each metal; (b) a NaOAc-buffered (pH = 5.2) aqueous mixed-metal solution with *ca.* 1.25 equiv. of each metal (*slightly lower for $UO_2^{2+}$ due to saturation concentration); (c) a NaOAc-buffered (pH = 5.2) aqueous mixed-metal solution with *ca.* 0.6 equiv. of each metal. (d) Representative $^{31}P\{^1H\}$ NMR spectrum of the DCE layer following post-X of $UO_2^{2+}$ from the aqueous, buffered mixed-metal solution (0.6 equiv.). No resonances attributable to $Cs^+$, $Nd^{3+}$, $Sm^{3+}$, or $Th^{4+}$ extraction are present. (e) Representative $^{31}P\{^1H\}$ NMR spectrum of the DCE layer following GBE and $UO_2^{2+}$ back-X to a fresh, buffered aqueous phase (*unknown by-product). (f) $^1H-^{13}C$ HSQC NMR spectrum of **[Bu$_4$N][$^{PO}$CbH]** in $CDCl_3$ revealing C1–H1 correlation. (g) Solid-state molecular structure obtained by XRD studies of **[Bu$_4$N][$^{PO}$CbH]** ($[Bu_4N]^+$ counter cation, phenyl C–H linkages, and all H atoms, except H1, are omitted for clarity).

peaks (28%) (*vide infra*, Fig. 3d). The main new resonance at 52.0 ppm in DCE matches the chemical shift of the *bis*-carborane complex, **[CoCp*$_2$]$_2$[UO$_2$($^{PO}$Cb)$_2$]**, in MeCN-$d_3$ and referenced to $[PPN]^+$ (this salt is insoluble in DCE). Given that the calculated ICP-OES-determined quantity of captured $UO_2^{2+}$ is 0.50 equiv. and 0.49 equiv. relative to the electrochemically generated $^{PO}$**Cb**$^{2-}$ (1.0 equiv.) for the buffered 1.25 equiv. (Fig. 3b) and 0.60 equiv. (Fig. 3c) reactions, respectively, we propose that the resonance at 52.0 ppm most likely represents the *bis*-ligated anion, **[UO$_2$($^{PO}$Cb)$_2$]$^{2-}$**. Together, these results indicate that electrochemically generated $^{PO}$**Cb**$^{2-}$ *selectively* captures $UO_2^{2+}$ from a mixed alkali, lanthanide, and actinide aqueous phase. While the nature of this selectivity remains under investigation, we suspect that optimal covalent bonding interactions between the P=O units and the U center – very recently investigated in the PUREX context[29,30] – are likely at play.

In addition to this selective capture, these biphasic experiments revealed the formation of minor byproduct resonances in the $^{31}P\{^1H\}$ NMR spectrum of the DCE phase at 28.6 and 25.8 ppm (Fig. 3d). These resonances consistently had a 1 : 1 ratio suggesting that this may be a single product with inequivalent P centers. We also observed that these resonances became dominant when mixing a DCE solution of $^{PO}$**Cb**$^{2-}$ with an aqueous buffered phase in the absence of additional metal. Thus, treatment of a DCE solution containing **[Bu$_4$N]$_2$[$^{PO}$Cb]** to the NaOAc-buffered aqueous solution *without* additional metals cleanly generated the byproduct, along with residual $^{PO}$**Cb**. The unknown byproduct was isolated by separation of the DCE phase, removal of the solvent, and selective crystallization by vapor diffusion of pentane into a saturated THF solution of the crude mixture. Analysis of the colorless single crystals by XRD studies revealed the formation of the protonated, monoanionic carborane species, **[Bu$_4$N][$^{PO}$CbH]** (Fig. 3g), featuring protonation at one of the *nido*-carborane C centers. The H1 atom at C1 was located in the difference map and was further observed by $^1H$ and $^1H-^{13}C$ HSQC NMR spectroscopy (Fig. 3f). The distinctly different geometries at C1 *versus* C2 leads to the observed asymmetry in the product and is responsible for the distinct $^{31}P$ NMR resonances observed. To the best of our knowledge, this is the first example of protonation of the *ortho*-substituted *nido*-carborane unit, $[1,2\text{-}L_2\text{-}1,2\text{-}C_2B_{10}H_{10}]^{2-}$, at one of its C centers.

The release of extracted $UO_2^{2+}$ was next probed electrochemically (Fig. 1b). The DCE phase containing the extracted $UO_2^{2+}$ was separated from the aqueous phase and returned to the H-cell where it was galvanostatically discharged to achieve a theoretical final SOC of *ca.* 0% (Fig. S6†). The DCE layer was next removed from the H-cell and a fresh, buffered (0.1 M NaOAc) or non-buffered aqueous solution was mixed with it rapidly for 15 h. Analysis of the aqueous layer by ICP-OES revealed the back-X of 22–38% of $UO_2^{2+}$ relative to post-X values, with similar values observed regardless of the use of

buffered or non-buffered aqueous solutions (Fig. 3a–c). The highest $UO_2^{2+}$ back-X observed were in the 0.6 equiv. separations (*ca.* 38%), wherein concurrent back-X of $Th^{4+}$ was also observed, albeit in smaller quantities (*ca.* 16%) relative to post-X (Fig. 3c). With the exception of this case, the back-X of all metals except $UO_2^{2+}$ was negligible compared to the controls. Further analysis of the DCE layer by $^{31}P\{^1H\}$ NMR spectroscopy revealed the conversion back to the starting *closo*-carborane, $^{PO}$**Cb** (Fig. 3e), as well as a minor unknown byproduct at 20.2 ppm (*ca.* 10% of total carborane peaks). These results demonstrate the electrochemical back-X of selectively captured $UO_2^{2+}$ to an aqueous phase.

## Conclusion

In summary, we have demonstrated the selective biphasic electrochemical capture and release of $UO_2^{2+}$ from mixed-metal aqueous media using the redox-switchable $^{PO}$**Cb**/$^{PO}$**Cb**$^{2-}$ system. This system may offer a unique, electrochemical, non-stoichiometric extraction platform – distinguished from current PUREX technology – for $UO_2^{2+}$ separation. Further studies are underway to further optimize this proof-of-principle system and to probe the origin of this selectivity, as well as to expand the mixed-metal system and better mimic SNF mixtures. New metal capture and release chemistry of energy importance is also being investigated.

## Data availability

All of the experimental data have been included in the ESI.† Crystallographic data can be obtained from the CCDC (2071514–2071518).

## Author contributions

M. K. synthesized and fully characterized all new complexes. M. K. and M. M. performed the biphasic electrochemical extraction experiments. M. M. performed all ICP-OES analyses. S.-L. Z. and G. W. performed all crystallographic refinements. T. W. H. provided some starting materials and assisted with data analysis. M. K., M. M., and G. M. wrote the manuscript with input from all authors. G. M. directed the research.

## Conflicts of interest

There are no conflicts to declare.

## Acknowledgements

We thank the National Science Foundation (CHE-1900651), the US-Israel Binational Science Foundation (2018221), and the US Department of Energy, Office of Basic Energy Sciences (DE-SC0001861, DE-SC0021649) for funding. The MRL Shared Experimental Facilities are supported by the MRSEC Program of the NSF under Award No. DMR 1720256; a member of the NSF-funded Materials Research Facilities Network (http://www.mrfn.org).

## References

1 IAEA, *Nuclear Power and the Paris Agreement*, https://www.iaea.org/sites/default/files/16/11/np-parisagreement.pdf, accessed 2/5/2021, 2021.
2 A. Adamantiades and I. Kessides, *Energy Policy*, 2009, **37**, 5149–5166.
3 D. J. Rose, *Science*, 1974, **184**, 351–359.
4 I. Kumari, B. V. R. Kumar and A. Khanna, *Nucl. Eng. Des.*, 2020, **358**, 110410.
5 W. B. Lanham and T. C. Runion, *Purex Process for Plutonium and Uranium Recovery (No. ORNL-479 (Del.))*, Oak Ridge National Lab, USA, 1949.
6 J.-P. Glatz, in *Comprehensive Nuclear Materials*, ed. R. J. M. Konings and R. E. Stoller, Elsevier, Oxford, 2nd edn, 2020, pp. 305–326.
7 P. Carbol, D. H. Wegen, T. Wiss, P. Fors, C. Jegou and K. Spahiu, in *Comprehensive Nuclear Materials*, ed. R. J. M. Konings and R. E. Stoller, Elsevier, Oxford, 2nd edn, 2020, pp. 347–386.
8 M. Keener, C. Hunt, T. G. Carroll, V. Kampel, R. Dobrovetsky, T. W. Hayton and G. Ménard, *Nature*, 2020, **577**, 652–655.
9 Y. Wu, X. Zhang, S.-Y. Kim and Y. Wei, *J. Nucl. Sci. Technol.*, 2016, **53**, 1968–1977.
10 M. A. Denecke, N. Bryan, S. Kalmykov, K. Morris and F. Quinto, in *Experimental and Theoretical Approaches to Actinide Chemistry*, ed. J. K. Gibson and W. A. Jong, Wiley, 2018, pp. 378–444.
11 F. Lahrouch, O. Sofronov, G. Creff, A. Rossberg, C. Hennig, C. Den Auwer and C. Di Giorgio, *Dalton Trans.*, 2017, **46**, 13869–13877.
12 P. A. Bingham, R. J. Hand, M. C. Stennett, N. C. Hyatt and M. T. Harrison, *MRS Online Proc. Libr.*, 2011, **1107**, 421.
13 A. E. V. Gorden, J. Xu, K. N. Raymond and P. Durbin, *Chem. Rev.*, 2003, **103**, 4207–4282.
14 N. S. Hosmane, T. Demissie, H. Zhang, J. A. Maguire, W. N. Lipscomb, F. Baumann and W. Kaim, *Organometallics*, 1998, **17**, 293–295.
15 A. R. Oki, O. Sokolova, B. Gilbes, A. Aduroja, G. Abdelaziz and T. J. Emge, *Inorg. Chem. Commun.*, 2002, **5**, 694–697.
16 R. Neufeld, R. Michel, R. Herbst-Irmer, R. Schöne and D. Stalke, *Chem. - Eur. J.*, 2016, **22**, 12340–12346.
17 A. I. Ojeda-Amador, A. J. Martínez-Martínez, A. R. Kennedy and C. T. O'Hara, *Inorg. Chem.*, 2016, **55**, 5719–5728.
18 J.-C. Berthet, M. Nierlich and M. Ephritikhine, *Polyhedron*, 2003, **22**, 3475–3482.
19 Z. Spichal, M. Necas, J. Pinkas and Z. Zdrahal, *Polyhedron*, 2006, **25**, 809–814.
20 K. Miyata, T. Nakagawa, R. Kawakami, Y. Kita, K. Sugimoto, T. Nakashima, T. Harada, T. Kawai and Y. Hasegawa, *Chem. - Eur. J.*, 2011, **17**, 521–528.
21 Y.-Z. Pan, Q.-Y. Hua, L.-S. Lin, Y.-B. Qiu, J.-L. Liu, A.-J. Zhou, W.-Q. Lin and J.-D. Leng, *Inorg. Chem. Front.*, 2020, **7**, 2335–2342.
22 I. Korobkov, A. Arunachalampillai and S. Gambarotta, *Organometallics*, 2004, **23**, 6248–6252.

23 A.-G. D. Nelson, T. H. Bray, F. A. Stanley and T. E. Albrecht-Schmitt, *Inorg. Chem.*, 2009, **48**, 4530–4535.
24 J. Diwu, J. J. Good, V. H. DiStefano and T. E. Albrecht-Schmitt, *Eur. J. Inorg. Chem.*, 2011, **2011**, 1374–1377.
25 F. Quilès, C. Nguyen-Trung, C. Carteret and B. Humbert, *Inorg. Chem.*, 2011, **50**, 2811–2823.
26 D. D. Pant and D. P. Khandelwal, *Proc. - Indian Acad. Sci., Sect. A*, 1959, **50**, 323–335.
27 C. Hunt, M. Mattejat, C. Anderson, L. Sepunaru and G. Ménard, *ACS Appl. Energy Mater.*, 2019, **2**, 5391–5396.
28 N. A. Thiele, D. J. Fiszbein, J. J. Woods and J. J. Wilson, *Inorg. Chem.*, 2020, **59**, 16522–16530.
29 D. Raychaudhuri, G. Gopakumar, S. Nagarajan and C. V. S. Brahmmananda Rao, *J. Phys. Chem. A*, 2020, **124**, 7805–7815.
30 Y. Zhang, W. Duan, Y. Yang, T. Jian, Y. Qiao, G. Ren, N. Zhang, L. Zheng, W. Yan, J. Wang, J. Chen, S. G. Minasian and T. Sun, *Inorg. Chem.*, 2022, **61**, 92–104.